ELSEVIER

1 December 1998

OPTICS COMMUNICATIONS

Optics Communications 157 (1998) 139–144

Ionization-induced pulse shortening and retardation of high intensity femtosecond laser pulses

S.P. Nikitin [a,*], Yuelin Li [a], T.M. Antonsen [b], H.M. Milchberg [a]

[a] *Institute for Physical Science and Technology, University of Maryland at College Park, College Park, MD 20742, USA*
[b] *Institute for Plasma Research, University of Maryland at College Park, College Park, MD 20742, USA*

Received 2 June 1998; revised 20 August 1998; accepted 24 August 1998

Abstract

High-intensity, ultrashort laser pulses were focused into a gas jet to study the propagation at intensities up to 10^{17} W/cm^2. The pulse intensity envelope and phase were measured using a modified version of the FROG (frequency-resolved optical gating) technique which allows an absolute time reference. Pulse shortening and retardation were observed and are explained by erosion of the leading part of the pulse due to ionization-induced refraction, and propagation of the remaining part of the pulse in the plasma. At sufficiently high pressures, multiple pulse formation followed by complete pulse break-up is observed. Numerical simulations are in qualitative agreement with experiment. © 1998 Elsevier Science B.V. All rights reserved.

Keywords: Ionization-induced pulse shortening; Ultrashort laser pulse; Gas jet

1. Introduction

The propagation of high intensity laser pulses in gases and plasmas is crucial in applications such as laser wakefield accelerators [1], X-ray lasers [2,17], and the fast ignitor concept for inertial confinement fusion [3]. In the interaction with a gas, an intense short laser pulse may experience substantial spatial and temporal distortions resulting from the ionization it induces. As a result, the peak intensity of the pulse may be reduced below the level required for applications.

Ionization-induced defocusing and spectral blue shifting have been studied theoretically and experimentally [4–7,18,8–11]. In recent work, spectral and spatial plasma-induced pulse distortions were studied using two-color pump-probe spectroscopy [10], or by investigating the spectra of third harmonic generated in the laser-gas interaction [11]. At best, the time resolution in this type of experiment is limited by the duration of the probe pulse. The recently developed FROG (frequency-resolved optical gating) technique [12] enables simultaneous monitoring of the pulse envelope and phase as a function of time with resolution of a few femtoseconds. Recently, the FROG technique was used to examine high intensity pulse propagation in aluminum plasmas [13,19], and the propagation of intense femtosecond pulses in preformed plasma channels [14].

This paper describes the use of a modified double-pulse FROG technique to measure pulse distortions associated with propagation of an intense laser pulse in an ionizing gas. In addition to providing the pulse envelope and phase evolution during gas ionization, the modified FROG provides an absolute time reference, achieved by using a reference pulse. At low gas densities ($< 2 \times 10^{18}$ cm^{-3}), we observed the erosion of the leading part of the pulse along with the retardation of its body, and at higher density, multiple pulse formation occurs followed by complete pulse break-up. The experimental results were compared with computer simulations based on a pulse propaga-

* Corresponding author. E-mail: snikitin@glue.umd.edu

0030-4018/98/$ - see front matter © 1998 Elsevier Science B.V. All rights reserved.
PII: S0030-4018(98)00473-8

tion code which includes field ionization and neutral gas $\chi^{(3)}$ effects.

The experiments reported here were performed with a 10 Hz Ti:Sapphire laser system, using 100 fs pulses with energy up to 15 mJ. Fig. 1 is a diagram of the experimental setup. The output of the laser was split with a pellicle (BS1) into a reference beam and a interaction beam ($>90\%$ energy). The reference pulse was propagated through an adjustable delay line. The interaction beam was focused with a $\sim f/8$ off-axis parabola (P) into a pulsed gas jet. The full width at half maximum (FWHM) of the laser focal spot in vacuum was ~ 8 μm, 1.6 times the diffraction limit. This resulted in peak vacuum intensities of $\sim 10^{17}$ W/cm^2. After the gas jet, the beam was recollimated and attenuated to an intensity level comparable to the reference beam. It was then recombined with the reference beam at beam splitter BS2 and directed to the FROG. We call this arrangement a time-domain interferometric FROG or TI-FROG. The TI-FROG trace contains both input and output pulse information, and provides both time and spectral fiducials. The technique allows measurement of the relative distortion of the interaction pulse and its absolute position on the time axis. The TI-FROG may be a simpler alternative to the recently proposed MI-FROG [15] for experiments where an absolute time reference is desired. In our experiment, the time separation between the reference and interaction pulses was adjustable in the ± 500 femtosecond range, a delay range which could be covered within a single shot FROG image without significant decrease in time resolution. We have previously performed radially resolved single pulse FROG measurements [14], but in the present experiment we restricted our observations to the axial direction.

The density profile of the gas jet was determined by comparing the images of spectrally and temporally integrated recombination emission from plasmas produced by lower intensity ($\sim 10^{16}$ W/cm^2) interaction with a gas jet and a static fill of known pressure. The emission yield was linearly dependent on the pressure of the static fill and the gas jet backing pressure. This is consistent with optical field ionization rather than avalanche as the dominant ionization mechanism for the short pulse width and low density of this experiment. At the interaction region 2 mm from the nozzle orifice, the density profile was a flat top distribution with a FWHM of ~ 2 mm and a full width of ~ 4 mm. The interaction was therefore in the tight focusing limit, with the Rayleigh length (~ 190 μm) of the pulse much smaller than the extent of the jet.

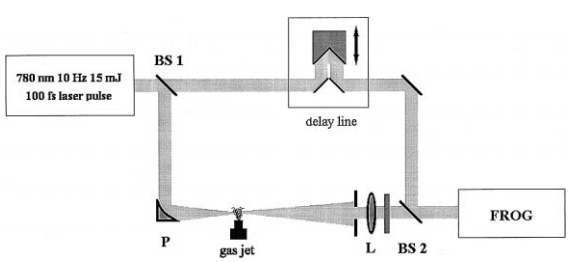

Fig. 1. Schematic of laser–jet interaction experiment, showing arrangement for time-domain interferometric FROG (TI-FROG).

In the experiment, we found even with poor alignment of the beamsplitters, the peak-to-peak separation between the reference and the interaction pulses could still be measured reasonably well directly from the TI-FROG trace. However, in order to ensure convergence of the FROG algorithm with acceptable accuracy, more careful alignment was necessary. In practice, sufficiently good alignment was achieved if the profile of the recombined beam at the output of BS2 contained no more than one interference fringe at zero optical delay between the reference and interaction beams.

A typical TI-FROG trace for the case of no gas is shown in Fig. 2(a), and the associated output from the FROG algorithm is shown in Fig. 2(b). In Fig. 2(a), the central portion contains the time domain interference fringes. The separation between the fringes is determined by the pulse separation. The side peaks are the cross-gated terms of the two pulses. From the retrieved pulse envelope and phase, it is seen that the pulses are very similar with reasonably flat phases as a function of time. Note that the reference pulse precedes the interaction pulse.

Fig. 2(c) shows a typical TI-FROG trace and Fig. 2(d) shows the recovered envelope and phase for interaction of a 10 mJ pulse with the He gas for a peak atom density of 1.4×10^{18} cm^{-3}. The reduced amplitude of the interaction pulse (the second pulse) is attributed to ionization-induced scattering of the light outside the detection solid angle. Also evident is an apparent erosion of the front of the pulse and a $\sim 30\%$ reduction in its FWHM. In comparison to the flat phase of the reference pulse, the target pulse also displays a constant decrease of phase beginning early in time. This results from self-induced ionization, leading to a frequency up-shift or blue shift $\Delta\omega(t) = -(\partial\Phi/\partial t)$, where $\Phi = \int kn \, \mathrm{d}l$ is the propagation phase, $n = 1 - N_e/2N_c$ is the plasma refractive index, k is the vacuum wavenumber, N_e is the electron density, N_c is the critical density and l is the distance along the propagation direction. Such blue shifts due to laser-induced ionization of gases have been well studied in previous experiments [4,5,10,11]. Figs. 2(e) and 2(f) show a typical TI-FROG trace and its recovered envelope and phase for gas density of 2.2×10^{18} cm^{-3}, where a blue shift and multiple pulse formation is evident. Beyond this density, the pulse appears to break up and the collected interaction pulse intensity begins to drop below the sensitivity level of the TI-FROG.

The measured FWHM and the average spectral shift of a 10 mJ interaction pulse in He as a function of peak gas density are given in Figs. 3(a) and 3(b) respectively. In Fig. 3(a) is also plotted the measured pulse retardation,

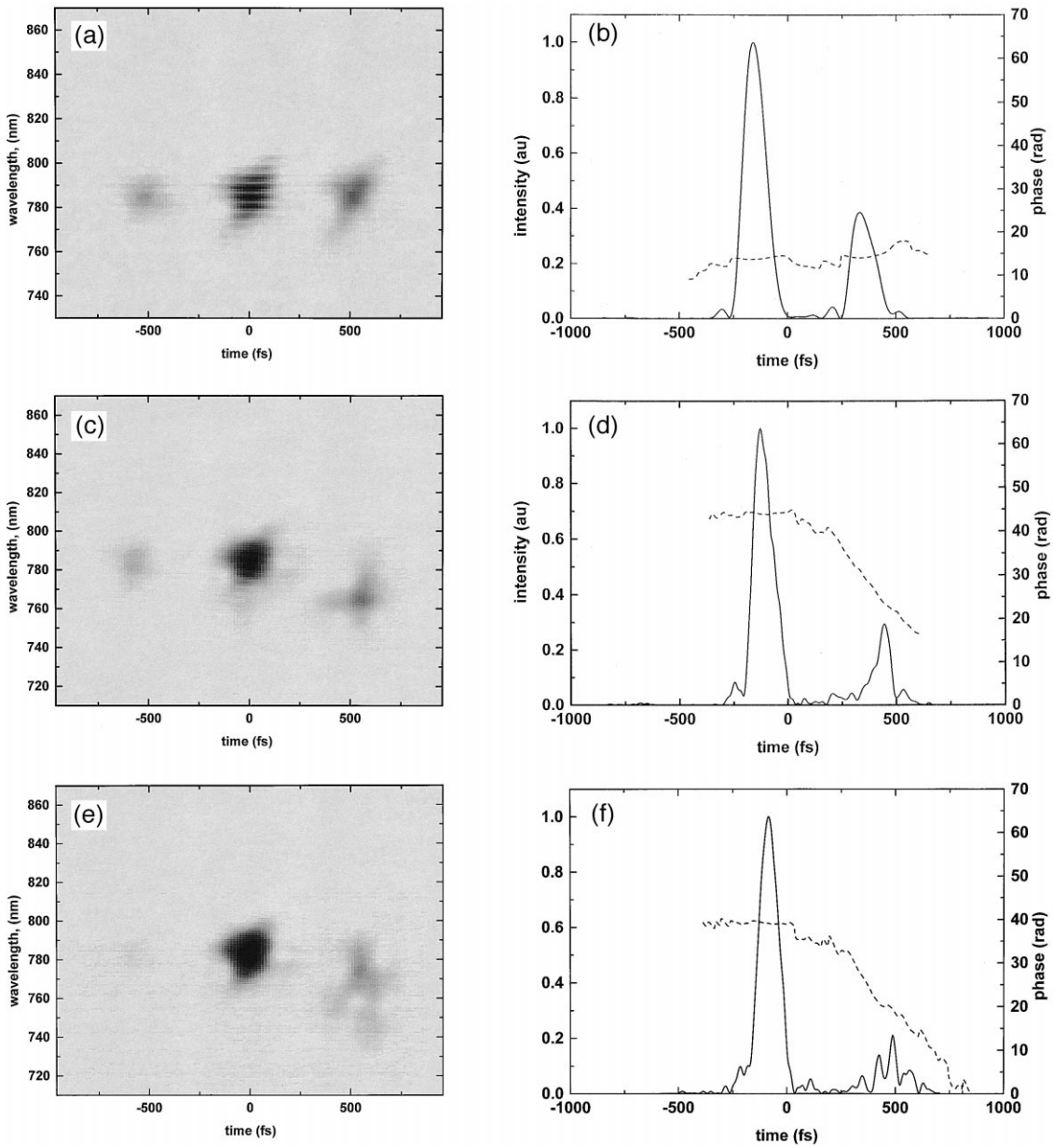

Fig. 2. (a) Typical TI-FROG trace (jet off), (b) envelope (solid line) and phase (dashed line) corresponding to (a); (c) TI-FROG trace (jet on, peak gas density of 1.4×10^{18} cm^{-3}), (d) envelope and phase corresponding to (c); (e) TI-FROG trace (jet on, peak gas density of 2.2×10^{18} cm^{-3}), (f) envelope and phase corresponding to (e).

which was found to accompany the blue shift and pulse shortening. The average spectral shift is obtained by subtracting the intensity weighted average wavelength of the reference pulse from that of the interaction pulse. The retardation was measured as the change in the peak-to-peak separation between the reference and interaction pulses. As can be seen in Fig. 3, with increasing gas densities up to 2×10^{18} cm^{-3}, the interaction pulse became more and more shortened and the retardation increased, accompanied by increasing blue shift. The interaction pulse duration shortened up to ~ 30 fs accompanied by a retardation of ~ 50 fs. For a double-ionized plasma produced in a path $l \sim 3$–4 mm of He gas at a density $\sim 2 \times 10^{18}$ cm^{-3}, the pulse retardation resulting from the group velocity in the plasma is $\Delta t = (l/c)(N_e/2N_c) \sim 10$–15 fs. We therefore identify the main contribution to the retardation (~ 20–30 fs) as erosion of the front of the interaction pulse, with the remainder (~ 10–20 fs) due to group delay in the plasma.

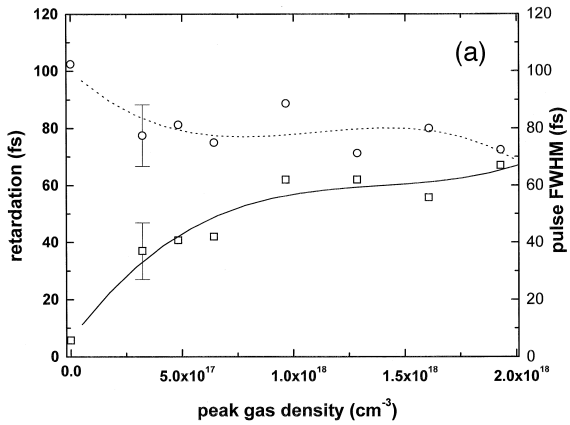

Fig. 3. (a) Output pulse FWHM (open circles) and retardation (squares) for incident 10 mJ pulse versus peak gas jet density; (b) pulse average spectral shift versus peak gas density. The lines are low order polynomial fits and the error bars represent the range of 5–10 shots at that density.

For the same range of densities of Fig. 3, we plot in Fig. 4 the output pulsewidth for target pulse energies of 5, 10 and 14 mJ, where it is seen that except for a general

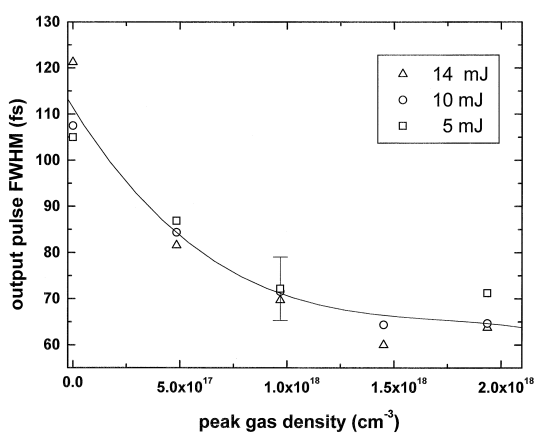

Fig. 4. Output pulse FWHM versus peak gas jet density for energies of 5, 10, and 14 mJ.

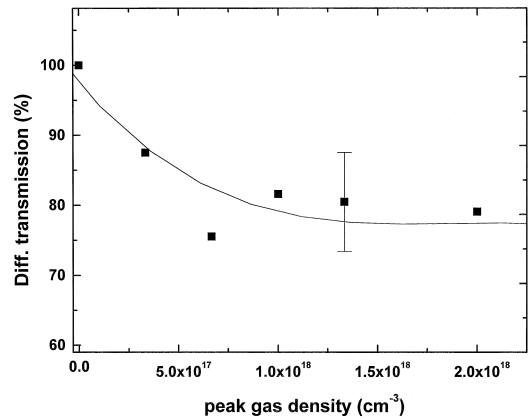

Fig. 5. Differential transmission along the optical axis of helium jet versus peak density for 10 mJ pulses.

trend to shorter pulses at higher pressure, there does not seem to be a clear energy dependence. In addition, no energy dependence of the retardation or average spectral shift could be identified within the accuracy of our measurement. Similar measurements performed with Ar showed that at lower density the results were qualitatively similar to helium: up to 30% pulse shortening for the same range of energies, with no clear trend in energy dependence.

For He densities higher than 2×10^{18} cm^{-3}, the interaction pulse distorted into an envelope with two or more peaks of comparable size, and our measure of pulse width and retardation was not as well-defined as at lower density. As mentioned earlier, at even higher densities, pulse breakup occurred and the on-axis intensity was below the sensitivity limit of the FROG measurement.

The TI-FROG traces also allow an estimation of the differential transmission for on-axis propagation of the interaction pulse, $T=(\mathrm{d}I_{\mathrm{out}}/\mathrm{d}\Omega)/(\mathrm{d}I_{\mathrm{in}}/\mathrm{d}\Omega)/_{\theta=0}$, defined as the ratio of laser flux scattered into a solid angle $\mathrm{d}\Omega$ centered around the propagation axis at the output of the gas jet to the input flux of the pulse. This is obtained by dividing the intensity integral of the interaction pulse by the intensity integral of the reference pulse, and normalizing by the ratio at zero gas density. The result for 10 mJ pulses for a range of density up to 2×10^{18} cm^{-3} is shown in Fig. 5. The $\sim$20% reduction in differential transmission is consistent with the observed pulse shortening and is therefore associated with the angular redistribution of the laser energy due to the refraction in the ionizing gas rather than absorption.

A simple picture of self-induced ionization allows qualitative understanding of the experimental results. For the tight focusing condition of this experiment, a lower energy pulse ($\sim$5 mJ, 6×10^{16} W/cm^2 at vacuum focus) begins ionization to He^+ at its temporal peak at a distance $\sim$1.5

mm before the focus. As the pulse continues to approach the focus and the intensity increases, the region of initial ionization moves forward on the pulse envelope, with the onset of ionization to He^{2+} lagging behind. The region of ionization starts as a narrow radial zone centered on the propagation axis and widens as the pulse approaches the focus, until its radial extent becomes a large fraction of the beam diameter. The change of refractive index over the gas-plasma transition results in a spectral blue shift due to self-phase modulation and defocusing in space due to refraction, which causes scattering to large angles of a large fraction of the front of the pulse. In comparison, a higher energy pulse (~ 15 mJ, 1.9×10^{17} W/cm^2 at the vacuum focus) begins ionization to He^+ immediately at the jet entrance before the pulse reaches its peak intensity, while ionization to He^{2+} begins ~ 0.8 mm before the focus at the pulse peak. The He^+ to He^{2+} transition region then moves forward on the pulse envelope, resulting in the refractive scattering of the front of the pulse. For observation in the far field on the optical axis, the scattered light is not detected and the remainder of the pulse, which propagates in already ionized gas, appears shortened. The insensitivity of the overall pulse shortening to pulse energy therefore partially results from the tight focusing geometry, where the transition to either He^+ or He^{2+} first occurs at the pulse temporal peak in advance of the focus, with the transition region advancing in the temporal envelope as the pulse approaches the focus.

To further understand details of the laser–gas jet interaction, we performed simulations using a laser pulse propagation model [16] which takes into account both the neutral helium gas optical nonlinearity ($\chi^{(3)}$) and optical field ionization. For these calculations the density profile of the gas jet was chosen to be trapezoidal with a 2 mm FWHM. The laser pulse at the focal plane in vacuum was modeled as $I(t) = I_0 \sin(\pi t/\tau) \exp(-2r^2/w_0^2)$, where $0 < t < \tau$ and τ was chosen so that the pulse was 100 fs FWHM. Consistent with the experimental focal spot intensity FWHM of 8 μm, the focal spot size was taken to be $w_0 = 6.8$ μm, for which the confocal parameter is $2z_0 = 363$ μm. In order to compare the results of the calculations with the experiment, the calculated pulse envelope and phase at the output plane of the jet (corresponding to the near optical field) was then used to calculate the far field envelope and phase. The calculated FWHM of the output pulse as a function of gas density is plotted in Fig. 6(a) for a range of pulse energies and gas jet densities, and the average wavelength shift is shown in Fig. 6(b). As can be seen, there is no clear trend in the output pulsewidth or blue shift versus energy, but the range of shortening and blue shift is in reasonable agreement with experiment (Figs. 3(a) and 3(b)). At gas densities higher than $\sim 2 \times 10^{18}$ cm^{-3}, the calculated target pulse begins to evolve into multiple pulses, in agreement with the experiments. Examination of the calculated electron density and laser field profiles shows that for these conditions there is no

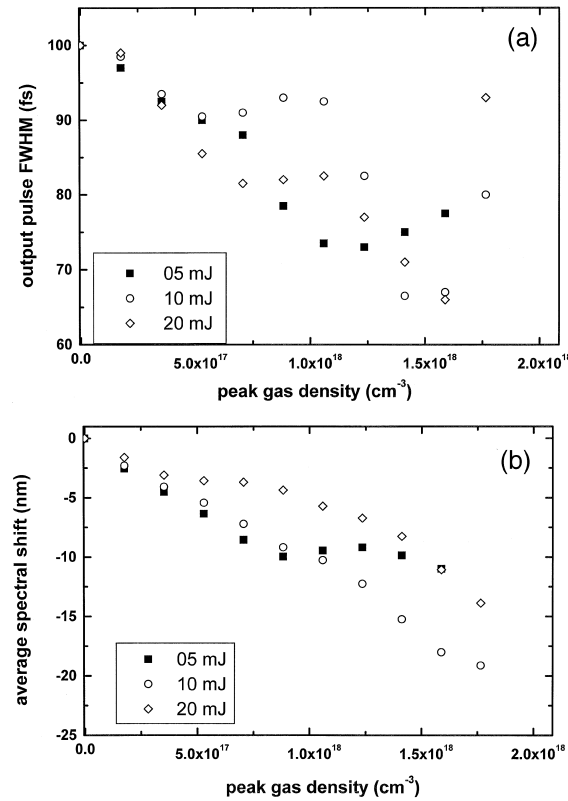

Fig. 6. (a) Calculation of output pulse FWHM versus peak gas jet density for energies in the range 5–20 mJ. Vacuum spot size $w_0 = 6.8$ μm, pulsewidth 100 fs; (b) calculated pulse average spectral shift versus peak gas jet density.

additional density modulation superimposed on the density profiles generated by optical field ionization of the jet, and that our observed multiple pulse formation and breakup is a phase effect resulting from interference among different time and space portions of the ionizing and refracting beam at high density. Pulse breakup resulting from plasma wake generation would have shown red shifts in the FROG traces, and only blue shifts were observed here. Indeed, the code confirms the well-known expectation that ionization-induced refraction reduces the maximum pulse intensity, here $\sim 10^{17}$ W/cm^2 in vacuum, which was already marginal for wake excitation.

In conclusion, by using TI-FROG measurements we have demonstrated the ability to measure ionization-induced amplitude and phase distortions of high intensity laser pulses with femtosecond time resolution. We find that the time-domain signatures that accompany blue-shifting and refraction are pulse shortening and retardation at low gas densities and multiple pulse formation at higher densities. Results of our numerical propagation code are in good qualitative agreement with experiment.

Acknowledgements

We acknowledge the support of the Department of Energy (DEF G0297 ER 41039).

References

[1] E. Esarey, P. Sprangle, J. Krall, A. Ting, IEEE Trans. Plasma Sci. 24 (1996) 252.
[2] B.E. Lemoff, G.Y. Yin, C.L. Gordon III, C.P.J. Barty, S.E. Harris, Phys. Rev. Lett. 74 (1995) 1574.
[3] M. Tabak, J. Hammer, M.E. Glinsky, W.L. Kruer, S.C. Wilks, J. Woodworth, E.M. Campbell, M.D. Perry, Phys. Plasmas 1 (1994) 1626.
[4] W. Wood, C.W. Siders, M.C. Downer, Phys. Rev. Lett. 67 (1991) 3523.
[5] S.P. LeBlanc, R. Sauerbrey, S.C. Rae, K. Burnett, J. Opt. Soc. Am. B 10 (1993) 1801.
[6] P. Monot, T. Auguste, L. Lompré, G. Mainfray, C. Manus, J. Opt. Soc. Am. B 9 (1992) 1579.
[7] S.C. Rae, Optics Comm. 97 (1987) 25.
[8] E.E. Fill, J. Opt. Soc. Am. B 11 (1994) 2241.
[9] A.J. Mackinnon, M. Borghesi, A. Iwase, M.W. Jones, G.J. Pert, S. Rae, K. Burnett, O. Willi, Phys. Rev. Lett. 67 (1996) 1473.
[10] S.P. LeBlanc, R. Sauerbrey, J. Opt. Soc. Am. B 13 (1996) 72.
[11] C.W. Siders, N.C. Turner, M.C. Downer, A. Babine, A. Stepanov, A.M. Sergeev, J. Opt. Soc. Am. B 13 (1996) 330.
[12] D.J. Kane, R. Trebino, Optics Lett. 18 (1993) 825.
[13] P.E. Young, P.R. Bolton, Phys. Rev. Lett. 77 (1996) 4556.
[14] S.P. Nikitin, T.M. Antonsen, T.R. Clark, Y. Li, H.M. Milchberg, Optics Lett. 22 (1997) 1787.
[15] C.W. Siders, A.J. Taylor, M.C. Downer, Optics Lett. 22 (1997) 624.
[16] P. Mora, T.M. Antonsen Jr., Phys. Plasmas 4 (1997) 217.
[17] Y. Nagata, K. Midorikowa, M. Obara, H. Tashiro, K. Toyoda, Phys. Rev. Lett. 71 (1993) 3774.
[18] S.C. Rae, Optics Comm. 104 (1994) 330.
[19] P.R. Bolton, A.B. Bullock, C.D. Decker, M.D. Feit, A.J.P. Megofna, P.E. Young, D.N. Fittinghoff, J. Opt. Soc. Am. B 13 (1996) 336.